

## Photoluminescence of Erbium-doped Silica-based Waveguide Film via Flame Hydrolysis Deposition and Aerosol Doping

Dongwook Shin\*

Division of Material Science & Engineering, Hanyang University, 17 Haengdang-dong, Seongdong-gu, Seoul 133-791, Korea

Silica based waveguides on Si fabricated by flame hydrolysis deposition were doped with erbium ions using an aerosol doping technique, and co-doped with GeO<sub>2</sub>, P<sub>2</sub>O<sub>5</sub> and B<sub>2</sub>O<sub>3</sub>. Erbium doping levels in the films were dependent on the nebulized solution concentration and delivery rate of the aerosol to the torch. The erbium solution concentration was varied from 4 to 8 wt%. The refractive index was measured by a prism coupler at 633 nm. FTIR absorption spectra and XRD profiles were made to check the OH concentration and the morphology of the films. A photoluminescence peak was observed at 1542 nm with a FWHM of 65 nm, which corresponds to the <sup>4</sup>I<sub>13/2</sub> → <sup>4</sup>I<sub>15/2</sub> transition. As a function of Er concentration, the photoluminescence (PL) intensity first increases, but decreases above a 6 wt% Er solution concentration. The decrease in PL intensity with concentration is attributed to concentration quenching caused by Er-Er interaction. The dependence of PL intensity on pump intensity further verifies the co-operative upconversion occurs.

**Key words:** Silica waveguide, Er-doped waveguide amplifier, Photoluminescence, 514 nm pumping.

### Introduction

Erbium is of particular interest because of an intra-4f transition with a wavelength around 1.5 μm, coinciding with a low-loss window of standard optical telecommunication silica fibers. An erbium-doped waveguide amplifier (EDWA) component can integrate waveguides, semiconductor diode lasers, and a variety of passive optical elements on a single chip, and it may thus provide a significant reduction in both device size and cost, desirable for all-optical local area networks. The potential for miniaturization of optical amplifiers has inspired considerable research interest in new Er<sup>3+</sup>-based amplifiers [1-7]. The restriction to compact (cm-scale) devices lengths in EDWA requires, in order to achieve sufficient net gain, much higher Er<sup>3+</sup> concentrations than the typical 100-300 ppm doping used in the several-tens-of-metres long EDFA. But this high concentration is responsible for a parasite effect caused by interactions between excited ions, notably co-operative upconversion and quenching by energy transfer.

Various methods have been used to fabricate EDWA [8-15], and in some cases optical gain has been demonstrated [16-18]. In this article, we used an aerosol doping technique to dope erbium in silica-based film co-doped with GeO<sub>2</sub>, P<sub>2</sub>O<sub>5</sub>, and B<sub>2</sub>O<sub>3</sub> fabricated by flame hydrolysis deposition (FHD).

An important advantage of this glass over other

materials is that low-loss-fiber-compatible planar waveguide can be fabricated by the standard silicon VLSI technology. A further advantage of using multicomponent glass is that it may accommodate larger erbium concentrations than pure silica. The aerosol doping technique has the advantage over the solution doping of incorporating the rare-earth ions into the glass in a single fabrication step during deposition, without the requirements to control the partial sintering temperature and to dry the sample after immersion [13]. Furthermore, The chemicals used are relatively inexpensive and the delivery system less complex in comparison with the method involving the vapor phase transport of rare-earth chelates [19, 20].

### Experiments

A schematic diagram of the FHD and the delivery system is given in Fig. 1. SiCl<sub>4</sub>, GeCl<sub>4</sub>, POCl<sub>3</sub> and BCl<sub>3</sub> were delivered to an oxy-hydrogen torch and hydrolyzed to form a low density soot, which was deposited on Si substrates with 1 μm thermally-grown SiO<sub>2</sub> on the silicon. Erbium ions were incorporated in the soot by feeding the torch with an aerosol of a solution of ErCl<sub>3</sub> (hydrous). An ultrasonic machine was used to atomize the solution. The Ar gas was used to deliver the resultant aerosol droplets to the torch. The refractive index and the thickness were controlled independently by changing the flow rate of the metal chloride and the number of traverses of the table. To consolidate the soot, samples were placed in a furnace and heated up to 1350°C.

The erbium concentration was dependent on the Ar

\*Corresponding author:  
Tel : +82-2-2220-0503  
Fax: +82-2-2299-3851  
E-mail: dwshin@hanyang.ac.kr

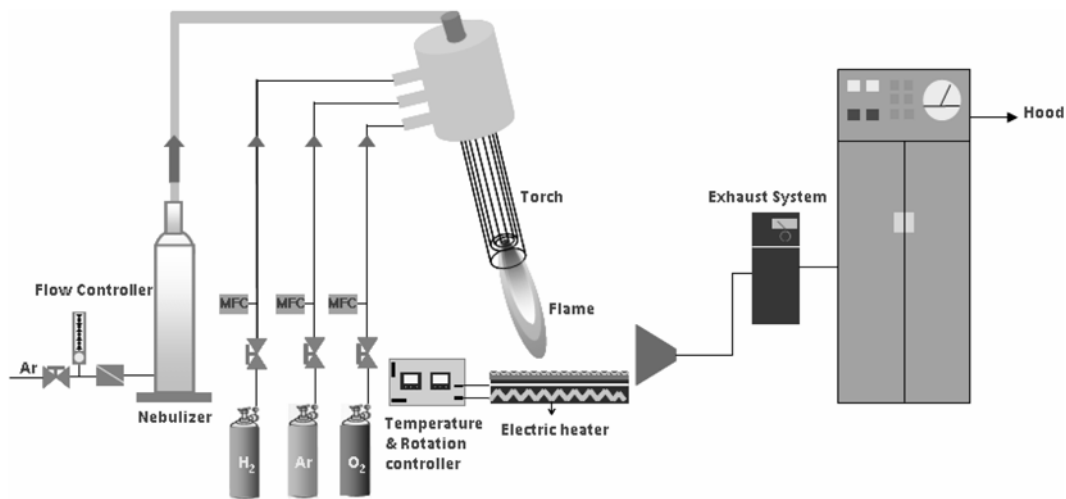


Fig. 1. Schematic diagram of the Flame Hydrolysis Deposition system and aerosol delivery system.

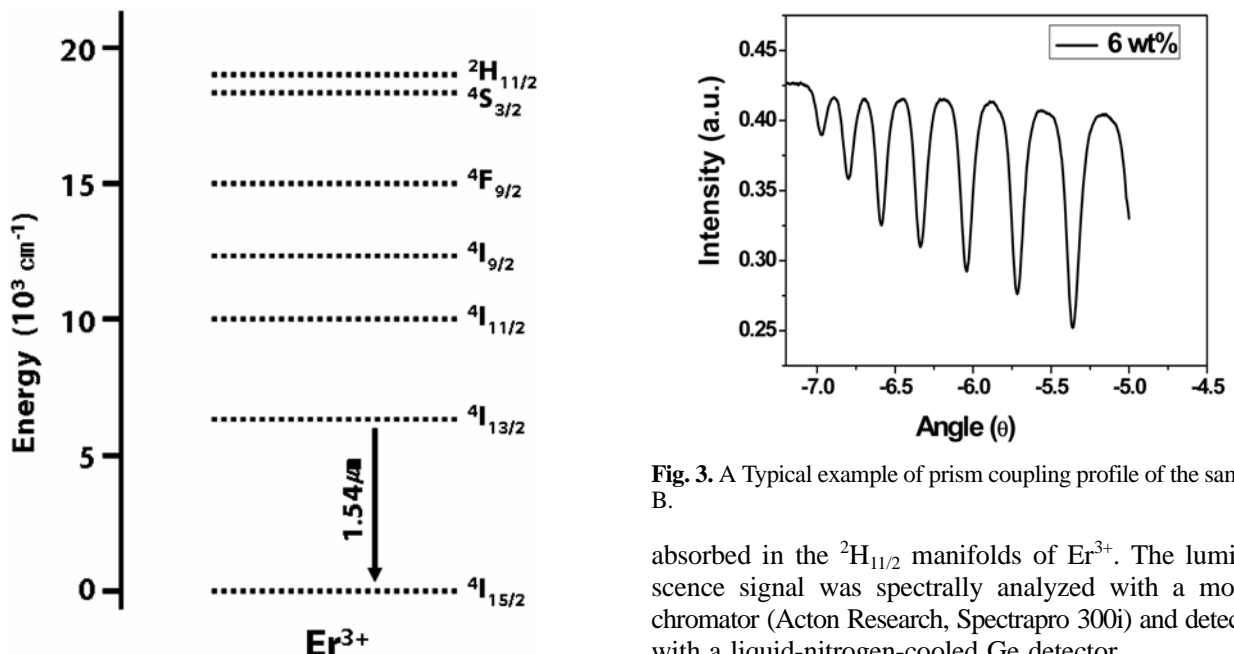


Fig. 2. Energy-level diagram of  $\text{Er}^{3+}$ .

gas flow rate, the ultrasonic resonator intensity and the erbium solution concentration. In this study, we fixed the Ar flow rate and the ultrasonic resonator intensity, and just changed the erbium solution concentration. (A: 4 wt%, B: 6 wt%, C: 8 wt%). The refractive index and the thickness of the erbium doped silica-based films were measured by a prism coupler (SAIRON Tech., SPA-4000) at a wavelength of 633 nm. FTIR (Nicolet, Magna 760) absorption spectra and XRD (Rigaku-Denki D/Max2500) profiles were obtained from these three planar waveguides to check the presence of OH in the films and the crystallinity of the films. Photoluminescence measurements were carried out at room temperature at 514 nm of an Ar-ion laser (Coherent, Innova 90C) as the excitation power source (see Fig. 2). This energy corresponding to the 514 nm line is

Fig. 3. A Typical example of prism coupling profile of the sample B.

absorbed in the  $^2\text{H}_{11/2}$  manifolds of  $\text{Er}^{3+}$ . The luminescence signal was spectrally analyzed with a monochromator (Acton Research, Spectrapro 300i) and detected with a liquid-nitrogen-cooled Ge detector.

## Results and Discussion

Figure 3 and Fig. 4 show the prism coupling profile of the sample B and the refractive index of erbium doped silica-based films, respectively. The refractive index difference  $\Delta$  was 2% between the films and the undercladding ( $n = 1.45$ ). This difference is higher than a typical silica passive waveguide ( $\Delta \approx 0.75$ ) and this high index difference leads to strong confinement of the mode fields, which can lower the required pump-power levels. The refractive index increased with increasing erbium solution concentration. In addition, with erbium concentration increases, the refractive index also increases.

Figure 5 shows the FTIR absorption spectra of the films in the planar waveguide and, within the sensitivity of our instrument, no characteristic bands of OH

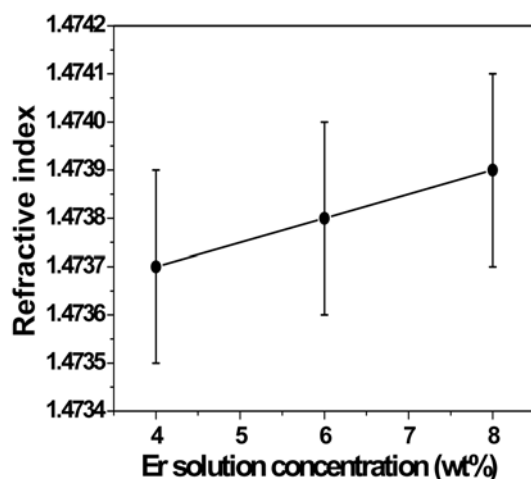


Fig. 4. The refractive indices of erbium-doped silica-based planar waveguide prepared by Flame Hydrolysis Deposition.

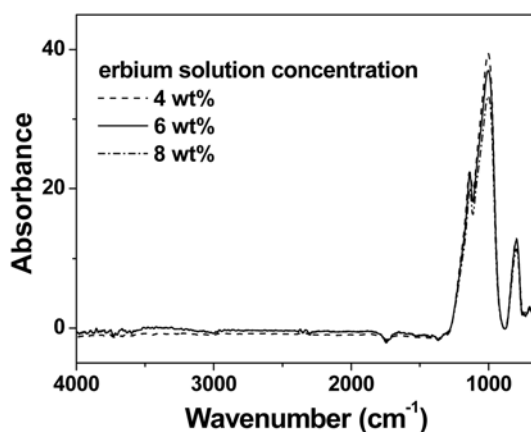


Fig. 5. FTIR spectra of the erbium-doped silica-based films prepared by Flame Hydrolysis Deposition.

group have been observed. Therefore, it may be concluded that the harmful OH group was successfully removed during the consolidation process.

Figure 6 shows the PL spectra of Er-doped silica-based films fabricated with different Er concentrations of the precursor solution. The spectra show peaks at the wavelengths of 1.542  $\mu\text{m}$  and 1.510  $\mu\text{m}$  and broad shoulders extending from roughly 1.45 to 1.65  $\mu\text{m}$  with the full width at half maximum (FWHM) of 65 nm. This emission is characteristic of the intra-4f transitions between the  $^4I_{13/2}$  and  $^4I_{15/2}$  manifolds of  $\text{Er}^{3+}$ . An additional peak was observed at wavelength 1.589  $\mu\text{m}$ . Figure 6 shows the PL peak intensity of sample B (6 wt% erbium solution concentration) was the highest among the samples measured at the set fixed experimental conditions.

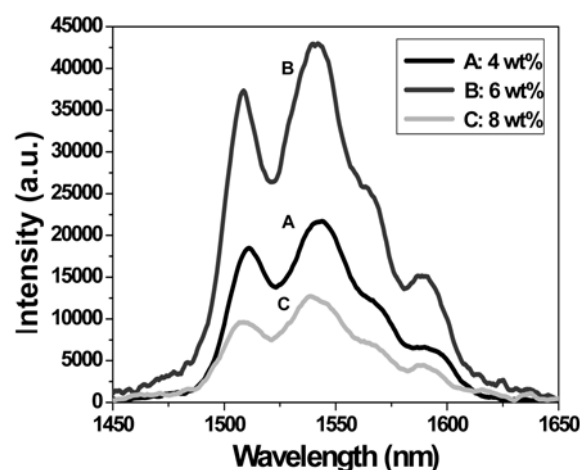


Fig. 6. Comparison of the photoluminescence intensity of the specimen of different erbium concentration of the precursor solution.

A pronounced peak was observed at 1.542  $\mu\text{m}$  with a FWHM of 65 nm, which is due to the transition between the different Stark level  $^4I_{13/2} \rightarrow ^4I_{15/2}$  manifolds, in combination with the homogeneous and inhomogeneous broadening. The  $^4I_{13/2}$  manifolds are populated through successive nonradiative relaxations from the  $^2H_{11/2}$  pump level.

Compared with the FWHM of the other glass (Table 1), the spectral width of our gain medium is clearly an advantage, because optical amplification is possible over a wide bandwidth for application in wavelength division multiplexed signal amplification. X-ray diffraction measurements show that the silica-based films are in an amorphous state (not shown). However, the curves of the PL spectra for  $\text{Er}^{3+}$  ion doped silica-based glass films are rather peaked. This peaky feature of the observed PL might suggest that the synthesized films contain some crystalline Er or  $\text{Er}_2\text{O}_3$  nano-particles due to the low vapor pressure of Er and early precipitation of this species in the flame.

An additional peak at 1.589  $\mu\text{m}$  was also observed. This peak is believed to lead to upconversion, because upconversion coefficients may be explained by the overlap between the  $^4I_{13/2} \rightarrow ^4I_{15/2}$  emission and the  $^4I_{13/2} \rightarrow ^4I_{9/2}$  absorption spectra, that is, the upconversion transition to the  $^4I_{9/2}$  manifold (800 nm) happens by the two-photon resonance of the peak emission wavelength from the  $^4I_{13/2}$  manifold (1600 nm) [21]. So we think the upconversion will occur in these samples as a result of a shoulder near to 1.6  $\mu\text{m}$ .

Generally, the decrease in PL intensity for high concentrations is attributed to energy migration in which the

Table 1. Comparisons of FWHM of  $\text{Er}^{3+}$  in several glass hosts

host	Bismuth-based	tellurite	silicate	Phosphate	Germinate	This study
FWHM (nm)	75	65	40	37	53	65

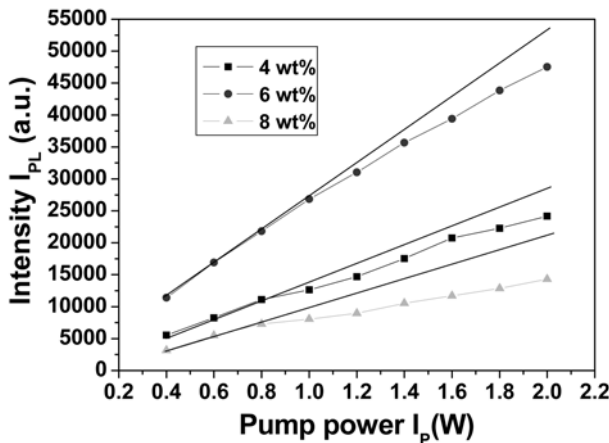


**Fig. 7.** Photoluminescence intensity at  $\lambda = 1.542 \mu\text{m}$  measured as a function of pump power at 514.5 nm. The samples were doped with the erbium concentrations of the precursor solution (4, 6, and 8 wt%).

excitation migrates by resonant exchange between closely spaced Er ions until the Er ions are strongly coupled to nonradiative quenching sites and co-operative upconversion in which energy is transferred nonradiatively from one excited Er ion to a neighboring excited Er ion, one is transferred to the ground state ( $^4I_{15/2}$ ) and another to the  $^4I_{9/2}$  level from which it rapidly relaxes to the metastable level ( $^4I_{13/2}$ ). It is well known that the second overtone of the OH stretch vibration is resonant with the transition from the first excited state to the ground state of Er. These effects have been studied in detail in other material doped with rare-earths [22, 23]. In this study, it is believed that the energy migration has little influence on the decrease of PL intensity due to the low OH concentration (FTIR spectra shown in Fig. 5), so the co-operative upconversion plays an important role.

In order to further investigate the co-operative upconversion, the dependence of the PL intensity on the pump power was measured. Furthermore, it is necessary to study the behavior as a function of pump power for future use of these highly-doped silica-based glasses films in EDWA. Because a silicate has a high phonon energy, the fraction of excited Er ions ( $N_2$ ) in a simple two level system pumped at a rate  $R$  is [24]:

$$N_2 = \frac{R\tau}{1+R\tau} \quad (1)$$

$$\text{where } R = \frac{I_p}{h\nu} \sigma_a$$

Here,  $h\nu$  is the energy of the pump intensity,  $I_p$  denotes the pump intensity and  $\sigma_a$  the absorption cross-section. It is well known that the lifetime decreases with an increase of erbium concentration. Equation 1 shows that  $N_2$  (the  $1.542 \mu\text{m}$  PL intensity) is sublinear in  $I_{PL}$  vs  $I_p$  and the sublinearity is less for samples with short lifetimes. Figure 7 shows the dependence of PL

intensity on pump power measured for three erbium solution concentration (4, 6, 8 wt%). The no dashed line on figure-solid the linear extrapolation of the first three data points. At higher pump intensities, the measured curves start to deviate from the linear extrapolation. However, in Fig. 7, the sublinearity with high concentration (short lifetime) is higher than with the low concentration (high lifetime). This suggests that co-operative upconversion related to both pump intensity and Er concentration takes place and it reduces the  $\text{Er}^{3+}$  population in the  $^4I_{13/2}$  manifolds and increases the pump power needed to obtain a certain degree of output. So the high erbium concentration has a high sublinearity. At the same time, Fig. 6 shows the additional peak at  $1.589 \mu\text{m}$  which verifies the presence of co-operative upconversion. In addition, the electrical dipole-dipole interaction probability between the different ions depends on the  $1/R^6$  [25], where  $R$  is the distance between two interacting ions. The energy migration and cooperative upconversion are forms of this interaction. So a high concentration has a low PL intensity and a bigger sublinearity due to the small distance between two ions.

## Conclusions

Erbium-doped  $\text{GeO}_2\text{-P}_2\text{O}_5\text{-B}_2\text{O}_3\text{-SiO}_2$  films fabricated by FHD and the aerosol technique show a clear photoluminescence around  $1.542 \mu\text{m}$  with a large FWHM of 65 nm. The refractive index difference can give higher confinement of mode fields. No characteristic peak of the OH group was observed from the FTIR spectra. The PL intensity first increases and then decreases with increasing erbium concentration which is attributed to the energy migration between the small-distance  $\text{Er}^{3+}$  ions and the co-operative upconversion. The co-operative upconversion quenching mechanism was further studied by the dependence of the PL intensity on the pump power. The presence of particles which have not been studied in this study will be investigated using TEM and XPS, and will be reported in a future publication.

## Acknowledgement

This work was supported by the Seoul Research and Business Development Program (Grant No. 10583).

## References

1. O. Lumholt, T. Rasmussen, and A. Bjarklew, IEEE Electron. Lett. 29 (1993) 495-496.
2. I. Massarek and P.F. Truoga, IEEE Photonics Technol. Lett. 5 (1993) 227-229.
3. E. Snoeks, G.N. van den Hoven, and A. Polman, J. Appl. Phys. 73 (1993) 8179-8183.
4. R.S. Quimby, W.J. Miniscalco, and B. Thopson, J. Appl. Phys. 76 (1994) 4472-4478.

5. H.K. Kim, C.C. Li, X.M. Fang, Y. Li, D.W. Langer, and J. Solomon, *J. Lumin.* 60-61 (1994) 220.
6. M. Federighi and F. DiPasquale, *IEEE Photonics Technol. Lett.* 7 (1995) 303-305.
7. E.D. Pasquale and M. Federighi, *J. Lightwave Technol.* 13 (1995) 1858-1864.
8. X.H. Zheng and R.J. Mear, *Appl. Phys. Lett.* 62 (1993) 793-795.
9. S. Honkanen, S.I. Najafi, P. Poyhonen, G. Orcel, W.J. Wang, and J. Chrostowski, *Electron. Lett.* 27 (1991) 2167-2168.
10. A. Polman, A. Ligard, D.C. Jacobsen, P.C. Becker, R.C. Kistler, G.E. Blonder, and J.M. Poate, *Appl. Phys. Lett.* 57 (1990) 2859-2861.
11. M. Nakazawa and Y. Kimura, *Electron. Lett.* 28 (1992) 2054-2056.
12. M.P. Hehlen, N.J. Cockroft, T.R. Gosnell, A.J. Bruce, G. Nykolak, and J. Shmulovich, *Opt. Lett.* 22 (1997) 772-774.
13. T. Kitagawa, K. Hattori, K. Shrito, M. Yasu, M. Kobayashi, and M. Horiguchi, *Electron. Lett.* 28 (1992) 1818-1819.
14. K. Shrito, K. Hattori, T. Kitagawa, Y. Ohmori, and M. Horiguchi, *Electron. Lett.* 29 (1993) 139-141.
15. W. Huang and R.R.A. Syms, *IEEE J. Lightwave Technol.* 21 (2003) 1339-1349.
16. Y.C. Yan, A.J. Faber, H. de Waal, P.G. Kik, and A. Polman, *Appl. Phys. Lett.* 71 (1997) 2292-2294.
17. R.N. Ghosh, J. Shmulovich, C.F. Kane, M.R.X. deBarros, G. Nykolak, A.J. Bruce, and P.C. Becker, *IEEE Photonics Technol. Lett.* 8 (1996) 518-520.
18. G.N. van der Hoven, R.J.I.M. Koper, A. Polman, C. van Dam, J.W.M. van Uffeien, and M.K. Smit, *Appl. Phys. Lett.* 68 (1996) 1886-1888.
19. R. Tumminelli, F. Hakimi, and J. Haavisto, *Opt. Lett.* 16 (1991) 1098.
20. K. Hattori, T. Kitagawa, M. Oguma, H. Okazaki, and Y. Ohmori, *J. Appl. Phys.* 80 (1996) 5301-5308.
21. E. Snoeks, G.N. van den Hoven, and A. Polman, *J. Opt. Soc. Am. B* 12 (1995) 1468.
22. Y.C. Yan, A.J. Faber, and H. de Waal, *J. Non-Cryst. Solids* 181 (1995) 283-290.
23. S.N. Houde-Walter, P.M. Peters, J.F. Stebbins, and Q. Zeng, *J. Non-Cryst. Solids* 286 (2001) 118-131.
24. E. Snoeks, G.N. van den Hoven, and A. Polman, *J. Appl. Phys.* 73 (1993) 8179-8183.
25. S. Sudo, "Optical Fiber Amplifier," Artech House Inc., (1997).